

Design of Chip-type Bandpass Filter Fabricated by LTCC

Guoan Wu¹, Xiaojun Bi¹, Qinghua Tang¹, Yao Cheng¹

¹Department of Electronic Science and Technology,
Huazhong University of Science & Technology, China

¹ Wuga5612@263.net

I. Introduction

In the RF wireless communication systems, high-performance, low-loss and compact size are the trends of passive integrated components^[1]. LTCC technology, as a novel multi-layer ceramic technology, with its high performance, high integration, high stability and low cost, has drawn wide attention in recent years. A fourth-order Chebyshev chip-type bandpass filter with a reasonable structure and stable performance is designed in this paper.

II. The circuit and the three-dimensional structure of filter

The main targets of this filter are as follows: center frequency of 2.45 GHz, passband of 2300-2600 MHz, ripple < 1 dB, VSWR in the passband < 1.4, stopband rejection > 40 dB ($f \leq 1700$ MHz and $f \geq 3700$ MHz). And the filter occupies an area of only $3.2 \times 1.6 \times 1.2$ mm³.

To get better effect of the stopband rejection, the initial structure of this filter utilizes small inductors and large capacitors^[2]. Equivalent circuit of the lumped-element fourth-order bandpass filter can be proposed as shown in Figure 1. The values of components in figure1 are as follows

$$L_1=1.01 \text{ nH}, C_1=3.48 \text{ pF}, C_2=0.79 \text{ pF}, C_3=2.99 \text{ pF}, C_4=0.48 \text{ pF}.$$

In this design, the four main kinds of elements adopted are as follows: resonant capacitor, coupling capacitor, resonant inductor and grounding inductor.

A. The resonant capacitor

As the resonant capacitor has a large value, the vertically integrated multilayer capacitor is adopted in the design^[3]. The detailed three-dimensional structure is shown in Figure 2.

B. The coupling capacitor

As shown in the Figure 3, the structure of general non-symmetric coupling resonator^[4] is adopted. Vertically integrated capacitor (VIC) topology was used to implement C_s , which is realized by two series capacitors with double capacitance. Each of this kind capacitors is implemented by a parallel combination of two capacitors with a value of C_s . This structure is depicted more clearly in the cross-sectional view in Figure 3.

Instance 1 in the figure 3(c) shows the offset condition between different layers. If the changed value of each C_s according to offset is ΔC , then the revised value of the total coupling capacitor C_s' will be as follows:

$$C_s' = \frac{2(C_s + \Delta C) \times 2(C_s - \Delta C)}{2(C_s + \Delta C) + 2(C_s - \Delta C)} = C_s - \frac{\Delta C^2}{C_s}$$

The error value of coupling capacitor is $-\Delta C^2/C_s$. Compared to traditional MIM capacitor structures, the error ΔC is greatly reduced of this design.

C. The resonant inductor

Only capacitive coupling is adopted in this filter design because inductive coupling is unnecessary. Needless inductive coupling can be eliminated by optimizing the three-dimensional structure of the filter. Meanwhile, as the size is very small, parasitic effect will increase and the insertion loss will rise if negative inductor is introduced to the adjacent resonators in this filter. To avoid these effects, via strip-line inductor is utilized. As can be

seen from figure 3(a), more distance will exist between vias according to the interlace-arranged form, and less mutual inductance and inductive coupling effect will be generated at the same time.

D. The grounding inductor L_g

The filter with capacitive coupling has poor rejection in the upper-stopband. The cross-coupling grounding inductor L_g can generate transmission zero and improve the stopband rejection. The equivalent circuit is shown in Figure 4.

When Y parameters of the modified filter with inductor L_g and Y parameters of the original filter have the same magnitude but the opposite phases, transmission zero will generate. The frequency of transmission zeros is mainly determined by the value of L_g .

When Y_{12} (or Y_{21}) of the whole filter schematic is equal to 0, the corresponding frequencies of two transmission zeros can be calculated

$$f_1 = 1.75 \text{ GHz} \quad f_2 = 4.02 \text{ GHz}$$

And the parameters of circuit are still as follows

$$L_1 = 1.01 \text{ nH}, C_1 = 3.48 \text{ pF}, C_2 = 0.79 \text{ pF}, C_3 = 2.99 \text{ pF}, C_4 = 0.48 \text{ pF}$$

The inductor L_g extracted from the three-dimensional structure is 0.011 nH. The simulation results are shown in Figure 5.

As can be seen from Figure 5, the rejection in the upper-stopband edge is significantly enhanced, which meets the design requirements.

The entire three-dimensional structure of filter is shown in Figure 6. Layer 1 and Layer 7 are the ground planes. Layer 2 and Layer 4 are connected by via form the grounding capacitor. The three interlayer coupling capacitors are realized on Layer 3. The grounding inductor L_g is the parasitic inductor between Layer 6 and Layer 7.

□. Test results and analysis

The samples fabricated by LTCC technology are shown in figure 7. The size is $3.2 \times 1.6 \times 1.2 \text{ mm}^3$. The dielectric constant of LTCC materials is 18.17 and the thickness of this ceramic sheet is 52.7 μm . By comparing curves, Figure 8 indicates that the test results from the network analyzer are basically matched to the simulation results. The test results are as follows: the ripple $< 1 \text{ dB}$, the VSWR < 1.4 , the stopband rejection $> 40 \text{ dB}$, and the insertion loss $< 2.5 \text{ dB}$, which meet the design targets well.

IV. Conclusions

A novel low temperature co-fired ceramic (LTCC) chip-type bandpass filter with the compact size is discussed in this paper. By the 3-D structural optimizing, the stability of the grounding capacitor and capacitive coupling coefficient is enhanced. In the meantime, the cross-coupling grounding inductor generates two transmission zeros, which bring better performance of the stopband rejection. The simulation of three-dimensional modeling and the experimental results are shown in this paper, test results indicated the experimental results have a good agreement with the simulation ones.

References

- [1] Lucero R.; Qutteneh W.; Pavio A.; Meyers D.; Estes J.; "Design of an LTCC switch diplexer front-end module for GSM DCS PCS applications", Radio Frequency Integrated Circuits (RFIC) Symposium, 2001. Digest of Papers. 2001 IEEE20-22 May 2001 Page(s):213 – 216.

- [2] L. K. Yeung and K. L. Wu, "A compact second-order LTCC bandpass filter with two finite transmission zeros," IEEE Trans. Microw. Theory Tech., vol. 51, no. 2, pp. 337–341, Feb. 2003.
- [3] J. Sheen, "LTCC-MLS duplexer for DCS-1800", IEEE Trans on Microwave Theory Tech, Vol 47, No 9, pp.1883-1889, September 1999.
- [4] Jia-Sheng Hong, M. J. Lancaster, Microstrip Filters for RF/Microwave Applications, John Wiley & Sons, 2001.

Figures

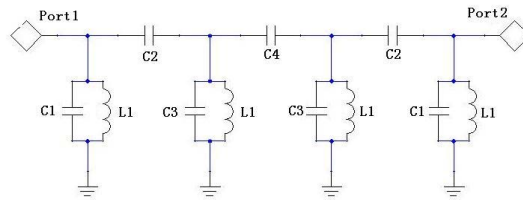


Figure 1. Circuit of the fourth-order bandpass filter

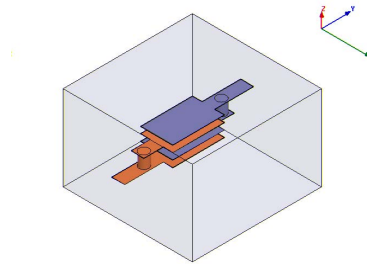


Figure 2. LTCC interlaced multilayer capacitor

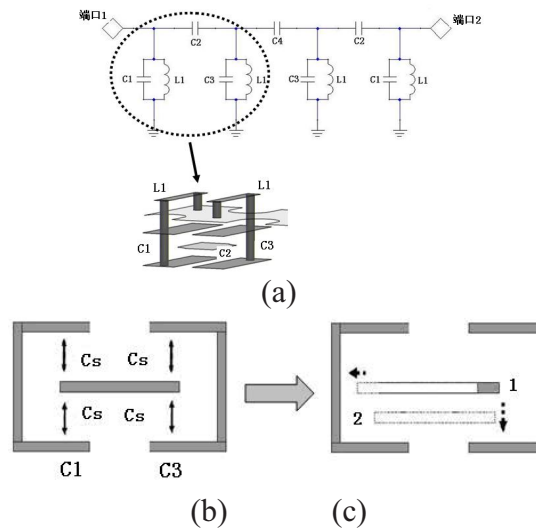


Figure 3. The three-dimensional structure of the coupling capacitor and coupling inductor
(a) The three-dimensional structure (b) The cross-sectional view (c) The offset

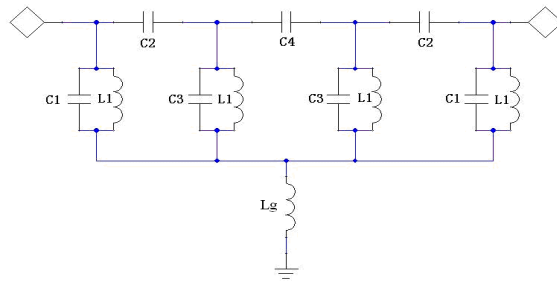


Figure 4. The circuit structure with grounding inductor

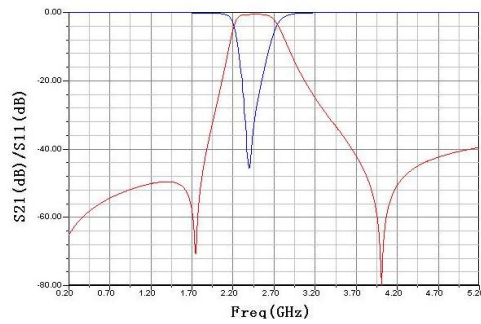


Figure 5. The simulation results with transmission zero

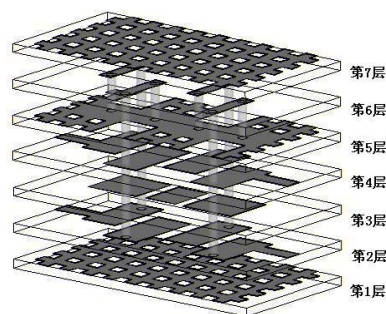


Figure 6. The three-dimensional structure of filter



Figure 7. The sample of the filter

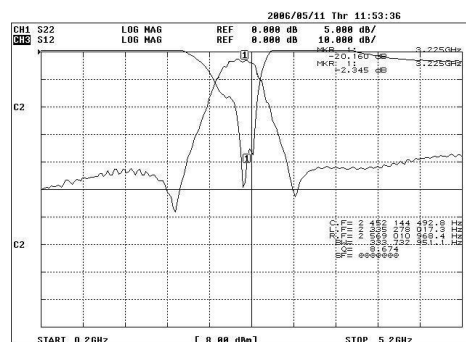


Figure 8. The test results from network Analyzer